

# Performance of an Anisotropic Magneto-Resistive Sensor

## Electrical Energy Meter

### ABSTRACT

This paper presents a digital electrical energy meter based on an Anisotropic Magneto-Resistive (AMR) current sensor and an Arduino micro microcontroller. This study aimed at designing and fabricating a digital electrical energy meter using the AMR sensor which overcomes some of the shortcomings of traditional current sensors used in most energy meters, display electrical energy, consumer's terminal voltage, supply current, power factor and „real-time“ power consumption. The study was carried out in the Department of Electrical and Control Engineering, Egerton University between September 2018 and December 2020. The meter was designed using Proteus 8 Professional software and fabricated on a printed circuit board. Algorithms were developed in C-language and stored in the microcontroller to continuously sample voltage and current signals derived from a successive supply voltage divider and the AMR current sensor, respectively. The sampling frequency was 2 kHz and every 10,000 samples were carried out to compute the Root Mean Square (RMS) values of voltage and current. The fabricated meter digitally computed the cumulative electrical energy in kilo-Watt-hours (kWhrs) and the other variables and displayed them on a 16×2 Liquid Crystal Display (LCD) after a consumption of every 0.01 kWhrs. Statistical results on the displayed variables indicated that the meters tested were not significantly different at 0.95 confidence level implying that those meters had similar performance. The extra displays are important and useful to power consumers and service providers in energy utilization and improvement of the quality of the power supplied. Power factor is an exceptional feature in the prototype meter beneficial to both consumers and power agencies in the decision-making process of reducing bills and power distribution costs leading to improved efficiency and service delivery.

**Keywords:** AMR current sensor, Arduino micro-microcontroller, Sampling, LCD, Electrically Erasable Programmable Memory

### ABBREVIATIONS

ACEEE	: American Council for an Energy-Efficient Economy
ADC	: Analogue to Digital Conversion
AMR	: Anisotropic Magneto-Resistive
AMRg	: Automatic Meter Reading
ANOVA	: Analysis of Variance
CT	: Current Transformer
EEPROM	: Electrically Erasable Programmable Memory
GMR	: Giant Magneto-Resistive
IEC	: International Electro-technical Commission
IOT	: Internet of Things
KEBS	: Kenya Bureau of Standards

kWhr	: kilo-Watt-hour
LCD	: Liquid Crystal Display
LSD	: Least Significant Different
MHz	: Mega-Hertz
OPAMP	: Operational Amplifier
PCB	: Printed Circuit Board
Pf	: power factor
RMS	: Root Mean Square
SAS	: Statistical Analysis of Systems
TMR	: Tunneling Magneto-Resistive

## 1. INTRODUCTION

Electromechanical meters have been used over a century and have been used in Kenya for over a century. They have an excellent combination of simplicity and reliability but lack the additional functionalities needed to integrate customers with a smart grid, such as real-time bills, range of measured quantities and communication capability. For these reasons, the transition to solid-state electrical energy meters has not therefore been one of choice, but of necessity as noted by Seal and McGranaghan [1].

Electrical energy meters may be classified into Electromechanical/induction, Electronic and Smart /Prepaid types as noted by Nwagbo and Baah [2]. Smart meters are basically electronic devices which measure the energy consumption regularly and report this to the consumers, utility companies and also third party service providers as reported by Aswathi *et al* [3]. A Prepaid energy meter enables power utilities to collect electricity bills from the consumers prior to its consumption [4]. Payments are made using tokens and power is cut off after the consumption of units paid for but restored automatically after another token is paid. Postpaid metering involves payment of energy consumed after usage as noted by Shomuyiwa *et al* [5].

An Automatic Meter Reading (AMRg) system consists of a consumption measurement, meter reading and data transmission, and data processing and billing as noted by Arun *et al* [6]. If meter data from the analogue input circuits is available in electronic form it becomes feasible to add communications to the meter, allowing the meter to use AMRg to access data remotely via a communication link [7]. This remote reading technique has the advantage of saving utility providers the expense of periodic trips to physical locations for meter readings [8].

The most common current sensors used for electricity metering devices are resistive shunts, Hall-effect sensors and current transformers as noted by Koon [9]. These sensors have several shortcomings which need to be addressed. Rogowski coil sensors are widely used in USA. Current transformers and current shunts have been used at the analogue inputs of modern wireless digital electrical energy meter having a microcontroller, a transmitter and a receiver with good results as reported by Ashiquzzaman *et al* [10]. Current measurement is considered to be more challenging because it requires a wider range of measurements and processing of a wider range of frequencies that are present in the current signal as reported by Volokhin *et al* [11]. This is partially due to numerous changes in electrical grid schemes, like the inclusion of renewable energy, the rise of non-linear loads and the emergence of electric vehicle charging systems which increase variable power quality conditions of the grid. This non-ideal power quality scenario produces an error in electricity meters that is not yet well known since there is no standardized procedure to calibrate meters under typical or emerging distorted waveform

conditions as reported by Cetina *et al* [12]. Voltage sensing is usually obtained by using either the voltage division method or a step down potential transformer as reported by Shahrara [13].

In one of the electronic meter designs by Hou and Yu [14], a resistance shunt is used as the current transducer while the voltage is acquired through a potential divider. The MSP430AFE is a slave-metrology processor while the MSP430F6638 is the host/application processor. The meter has a single decimal point display on an LCD. In another design by Hou and Yu [14], a current transformer (CT) and a resistance shunt are used for tamper detection in which the current in the live and neutral conductors are measured and compared. In yet another electronic meter design, Shahrara [13] used a Hall effect current sensor and a voltage transformer as the current and voltage signal transducers in the design of a microcontroller based wireless energy meter.

The accuracy of energy meters depends upon the various accuracies of the sensors used in the analogue input circuits, the sampling process, the Analogue to Digital Conversion (ADC) and digital calculations [15]. Despite well-developed traditional and alternate sources of electricity, there are many problems with regard to distribution, metering and billing of electrical energy and measurement of its consumption [10]. The American Council for an Energy-Efficient Economy (ACEEE) reviewed more than 36 different residential smart metering and feedback programs internationally. Their conclusion was that “to realize potential feedback-induced savings, smart meters must be used in conjunction with in-home displays and well-designed programs that successfully inform, engage, empower and motivate people” as reported by Kamilaris [16].

Electronic sensor market has experienced a rapid growth in recent years, driven by the Internet of Things (IoT). Sensors of various types are employed in multiple domains to sense and collect data, assisting in improving the production efficiency and facilitating our lives as reported by Shaohua Yan *et al* [17]. Most of the smart sensors required in smart living are in the field of spintronics. Based on distinct underlying mechanisms, spintronic sensors are normally categorized into Anisotropic Magneto-Resistance (AMR), Giant Magneto-Resistance (GMR), and Tunneling Magneto-Resistance (TMR) sensors [17]. Test results from Tunneling Magneto-Resistance TMR31 current sensor showed a linear relationship between its output voltage and current flowing through it with a sensitivity of 15.5 mV/A as reported by Enrique, *et al* [18].

The linear characteristics of the AMR resistor is achieved by the use of the barber pole structure in which the current is forced to flow in a direction  $45^\circ$  with respect to the magnetic field. Characteristic performance of current sensors in Table 1 [19] shows that the AMR current sensor possesses competing characteristics which could be exploited to design an accurate electrical energy meter with several advantages over traditional current sensors.

The ferromagnetic AMR sensor (19% Fe, 81% Ni) is manufactured using thin film technology as noted by Friedrich and Kunze [20]. It possesses intrinsic characteristics such as temperature stability, corrosion resistance, good electromagnetic properties, high reliability, small size and light weight and can be used in smart meters. Figure 2.5 shows a schematic diagram of an NT Series AMR sensor manufactured by F.W. Bell. The NT series current sensors have a high linearity (0.1%) and low temperature sensitivity, an output voltage  $V_{out} = \pm 2.5V$  at a nominal current  $\pm I_{PN}$ , a basic high accuracy of  $\pm 0.3\% I_{PN}$  and uses a surface area of (  $2.6cm^2$  ) on the PCB [20]. The sensor is only sensitive to measured current through the primary bus bar.

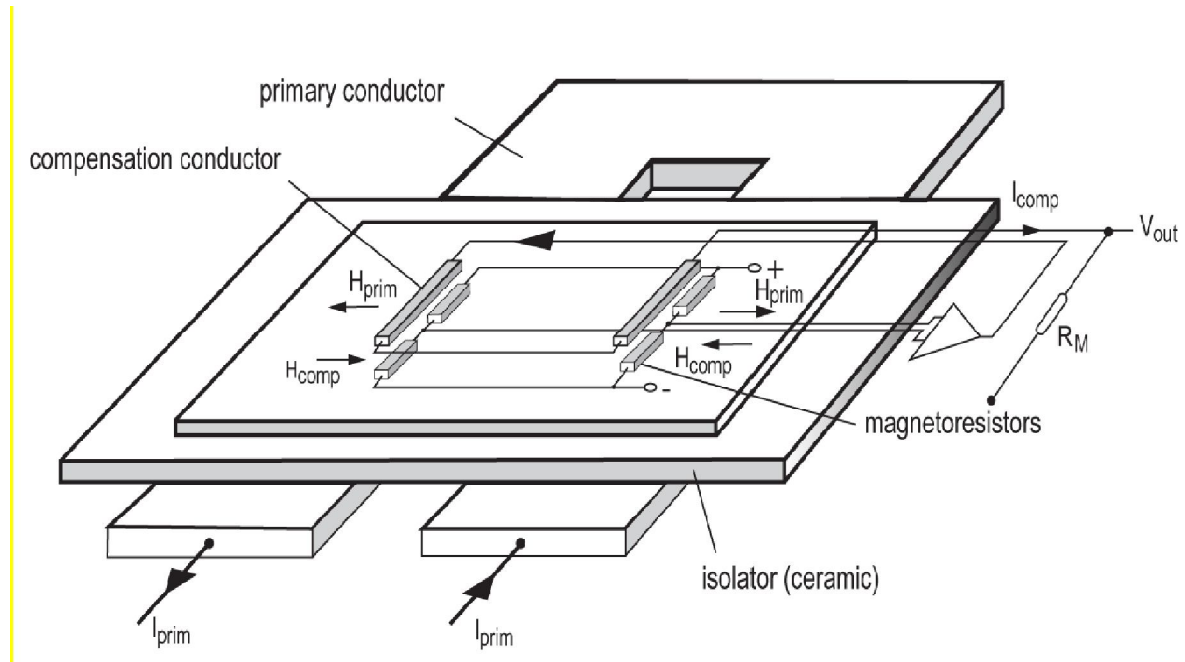


**Figure 1: Schematic diagram of an AMR sensor (Friedrich et al., 1999).**

Normally the sensor or transducer prices increase directly with their accuracy. To make the choice of the correct transducer, parameters like the final equipment price, the equipment performance and the application range must be considered as noted by Pinto [21].

**Table 1: Performance comparison of current sensors [18].**

Type of Sensor	Performance						
	Band-width	DC Capable	Accuracy	Thermal Drift	Isolated	Range	Power loss
Shunt resistor							
• Coaxial	MHz	Yes	0.1%-2%	25-300	No	kA	W-kW
• SMD	kHz-MHz					mA-A	mW-W
Copper Trace	kHz	Yes	0.5%-5%	50-200	No	A-kA	mW
Current Transformer	kHz-MHz	No	0.1%-1%	<100	Yes	A-kA	mW
Rogowski	kHz-MHz	No	0.2%-5%	50-300	Yes	A-MA	mW
Hall Effect (open loop, core-less)	kHz	Yes	0.5%-5%	50-1000	Yes	A-kA	mW
Fluxgate	kHz	Yes	0.001%-0.5%	<50	Yes	mA-kA	mW-W
AMR Effect (Closed loop, Core-less)	kHz	Yes	0.5%-2%	100-200	Yes	A	mW
Coreless, open loop(GMR, AMR, Hall Effect)	kHz	Yes	1%-10%	200-1000	Yes	mA-kA	mW
Fiber-optic Current sensor	kHz-MHz	Yes	0.1%-1%	<100	Yes	kA-MA	W

The high digital accuracy in electronic meter designs contributes very significantly to the overall meter accuracy. Despite new developments in digital sampling, processing and display,

transmission, billing and data management, development of new current sensors suitable for energy meters has remained behind. New technologies have been used to develop new current sensors which can be used in the production of possibly more accurate electronic energy meters. One of these sensors is the Anisotropic Magneto-Resistive (AMR) current sensor which has some advantages over the traditional sensors.

Through this research, a new meter that uses an AMR current sensor has been developed. The meter displays the consumer's terminal voltage, current drawn by the consumer's load, power factor, „real-time“ power consumption and the usual energy consumption. This acts as a part solution to the problems which arose during the review of smart meter applications by ACEEE. By monitoring the consumer's power factor and improving it appropriately, the customers would pay reduced bills for the same loads and also improve the overall power system power factor. This would effectively reduce the current drawn from the power distribution and transmission systems, the weight of the overhead lines and cables, the system  $I^2R$  power loss, the cost of switch-gear, construction, maintenance and labour. The surplus power would be used to improve customer connectivity. The power supply companies could also benefit by monitoring the power service from the meter displays at the consumer terminals.

This paper presents the performance of an electrical energy meter using an AMR current sensor. The current sensor gave a proportional output voltage of current flowing through it. The load voltage signal was derived from a resistive potential divider network. The voltage and current signals were sampled and processed by an Arduino micro microcontroller. A C-code program was written and stored in the EEPROM of the microcontroller to sample the consumer's terminal voltage and load current signals and process them to compute the terminal voltage, load current, „real-time“ power consumption, apparent power, power factor and the electrical energy consumed over a consumption period. All the variables (except the apparent power) were displayed on a 16×2 Liquid Crystal Display (LCD) after a consumption of every 0.01 kWhrs.

## **2. MATERIALS AND METHODS**

### **2.1 Testing the AMR current sensor**

The first experiment was to test the Anisotropic Magneto-Resistive current sensor. This experiment was carried out to obtain the output/input characteristics of the sensor. The currents drawn by the load and the output voltages of the sensor were recorded. The load was a combination of 1.22M×36W fluorescent fittings and 100W incandescent bulbs. The results are given in section 3.

### **2.2 Development of Prototype meter**

This study aimed at designing and fabricating a digital electrical energy meter which would display on a Liquid Crystal Display (LCD) the supply current, consumer's terminal voltage, power factor, real-time power consumption and electrical energy. The current and voltage signals were respectively derived from an AMR current sensor and supply voltage through resistive voltage division and suitable signal conditioning circuits. The electrical energy meter was designed using Proteus 8 Professional software. The Printed Circuit Board (PCB) was fabricated in the Department of Electrical and Control Engineering, Egerton University. The components

were then soldered to the PCB. A code was written in C-language and stored in the Microcontroller's EEPROM for processing the signals from which the other variables were derived. The fabricated electrical energy meter was then tested against selected meters from the market.

### 2.2.1 Block diagram of implemented electrical energy meter

Figure 2 shows a block diagram of the implemented digital electrical energy meter. It has the following sections: analogue signal acquisition which contains the voltage and current sensors, voltage and current signal conditioning section which contains appropriate amplifiers, Arduino micro microcontroller which does the digital sampling, processing and computations of necessary variables for display on the LCD display. The DC power supply of  $\pm 12V$  and  $+5V$  are not shown. The voltage divider network consists of a successive resistor arrangement that has a scaled down output voltage proportional to the consumer's terminal voltage. Successive approximation output voltages are available from the resistive network for calibration purposes. The load current flows through the AMR current sensor that outputs a voltage signal which is 10% of the value of the current and proportional to the load current.

The voltage and current signal conditioning circuits produce proportional and suitable signals to the microcontroller for sampling. The microcontroller samples the voltage and current signals and computes the supply current, voltage, power consumption, power factor and electrical energy which are sent to the LCD for display.

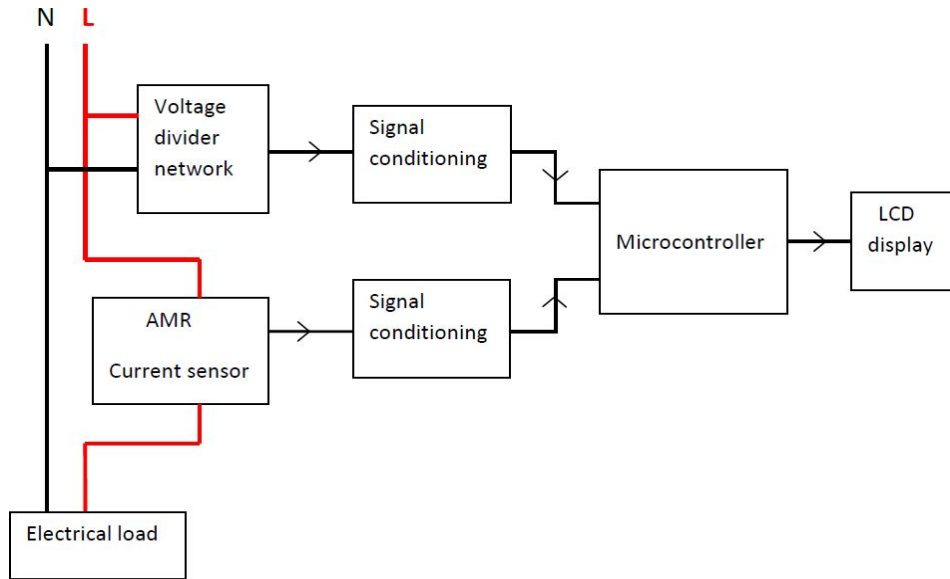


Figure 2: Block diagram of electrical energy meter

### 2.2.2 Signal Conditioning Circuits

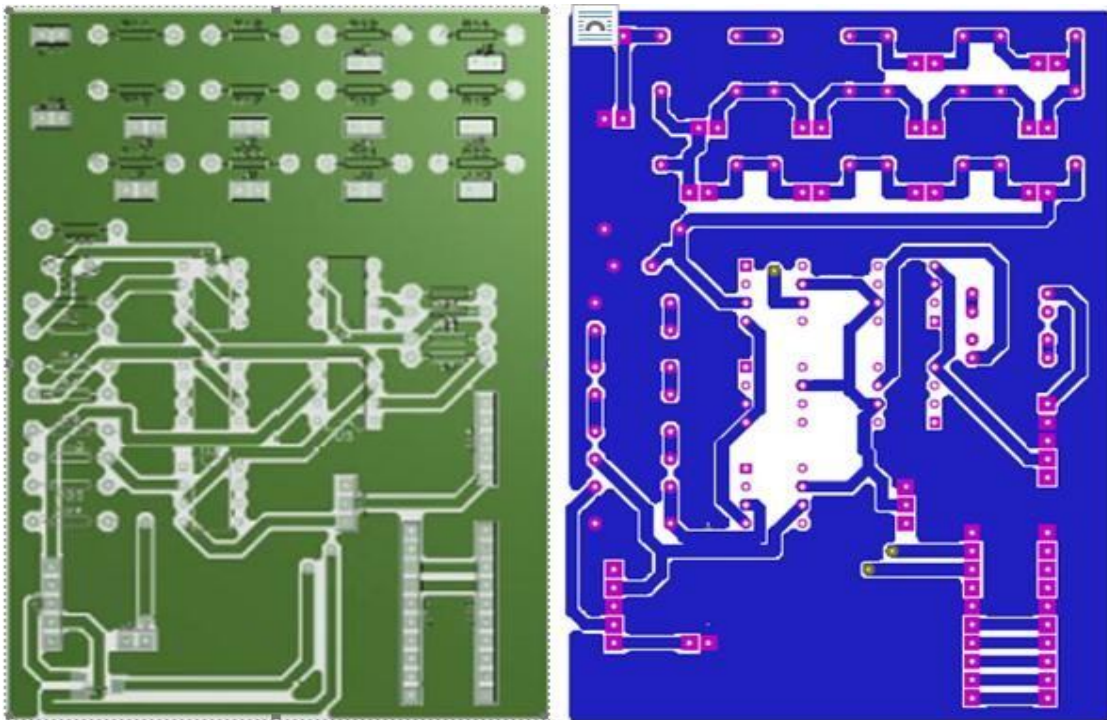
The meter was designed to operate off 240V 50 Hz power supply and the load current was limited to 25A (RMS) because of the limited rating of the available AMR current sensor. The voltage divider network was divided into 3 parts. The first part had  $2 \times 330k\Omega$  resistors and the second had 10 resistors whose values decreased approximately in successive divisions by 2 down to  $660 \Omega$  but with switched wire jumpers across each of them. The third part had a resistor of  $660\Omega$  with a  $10nF$  capacitor across it to provide a low-pass filter for supply signals up to the 20<sup>th</sup>

harmonic as required by International Electro-technical Commission (IEC). The output across the  $660\Omega$  was  $239.76\text{mV}$  ( $\approx 240\text{mV}$ ) for an input voltage of  $240\text{V}$ . This output was passed through a suitable voltage signal conditioning circuit to provide the required current signal to Arduino micro microcontroller for sampling.

The maximum voltage from the  $25\text{A}$  current sensor would be  $2.5\text{V}$  (RMS) or a peak-to-peak value of  $2 \times \sqrt{2} \times 2.5\text{V} = 7.0711\text{V}$ . At this rated current, an undesirable negative peak value of  $3.5355\text{V}$  would be available at the microcontroller terminals. This voltage would not be suitable for the Arduino because it works only with positive voltages and can't exceed its supply voltage of  $+5\text{V}$ . To avoid this possibility, the output voltage was divided by 2 and then passed through a suitable signal conditioning circuit to provide a proportional voltage for sampling. A „DC offset“ voltage of  $2.31\text{V}$  was provided to „lift“ the voltage and current signals to avoid the possibility of negative signal voltages appearing at the microcontroller's terminals. A power supply of  $\pm 12\text{V}$  supplied the AMR current sensor and the OPAMPS used in signal conditioning while the  $+5\text{V}$  supplied the Arduino micro and the LCD. A schematic diagram showing the assembly of the hardware was drawn using Proteus 8 Professional software and implemented on a Printed Circuit Board (PCB).

### 2.2.3 Development of hardware

Proteus 8 Professional software was used to draw the schematic diagram and the top and bottom layers of the PCB as shown in Figures 2 (a) and (b). The layers were printed on PCB paper and the image transferred to a double-sided copper-plated board. The actual PCB layouts were produced through an etching process. The PCB layouts have green and blue areas which represent the copper that remained after etching. The conducting paths (green and blue) have end terminations. The hardware components were then soldered on the etched board.



a) PCB top layer.

(b) PCB bottom layer.

**Figure 3: PCB top and bottom layers without components**

## 2.2.4 Development of software

The flow chart used to develop the software for computing the variables required are shown in Figure 4. The signal conditioning circuits were designed such that at zero-value inputs, the microcontroller terminals were at a „dc offset“ of 2.31V. At any instant, the voltage signals to be sampled by the microcontroller would be the actual voltage less the „dc offset“ voltage.

The clock frequency of the microcontroller was 16 MHz. A test run showed that it took 232 $\mu$ s to complete an ADC conversion for 1 pair of current and voltage samples. To obtain a high accuracy on computed data, a sample size of 10000 samples was selected.

The C-code program was written to sample a pair of current and voltage signals, perform ADC conversion and store the data in EEPROM of the Arduino. Using a sampling frequency of 2 kHz, this would take 0.5ms and 40 ADC conversions would be completed in 1 cycle. To obtain instantaneous values of consumed power, the two values would be multiplied and the result stored. To save the storage space, only the new sum was stored. The square root of the average of the sum of the squares of the ADC values of current and voltage would give the Root Mean Square (RMS) values of the current and voltage for the 10000 samples. These values would be used to calculate the apparent power and the power factor.

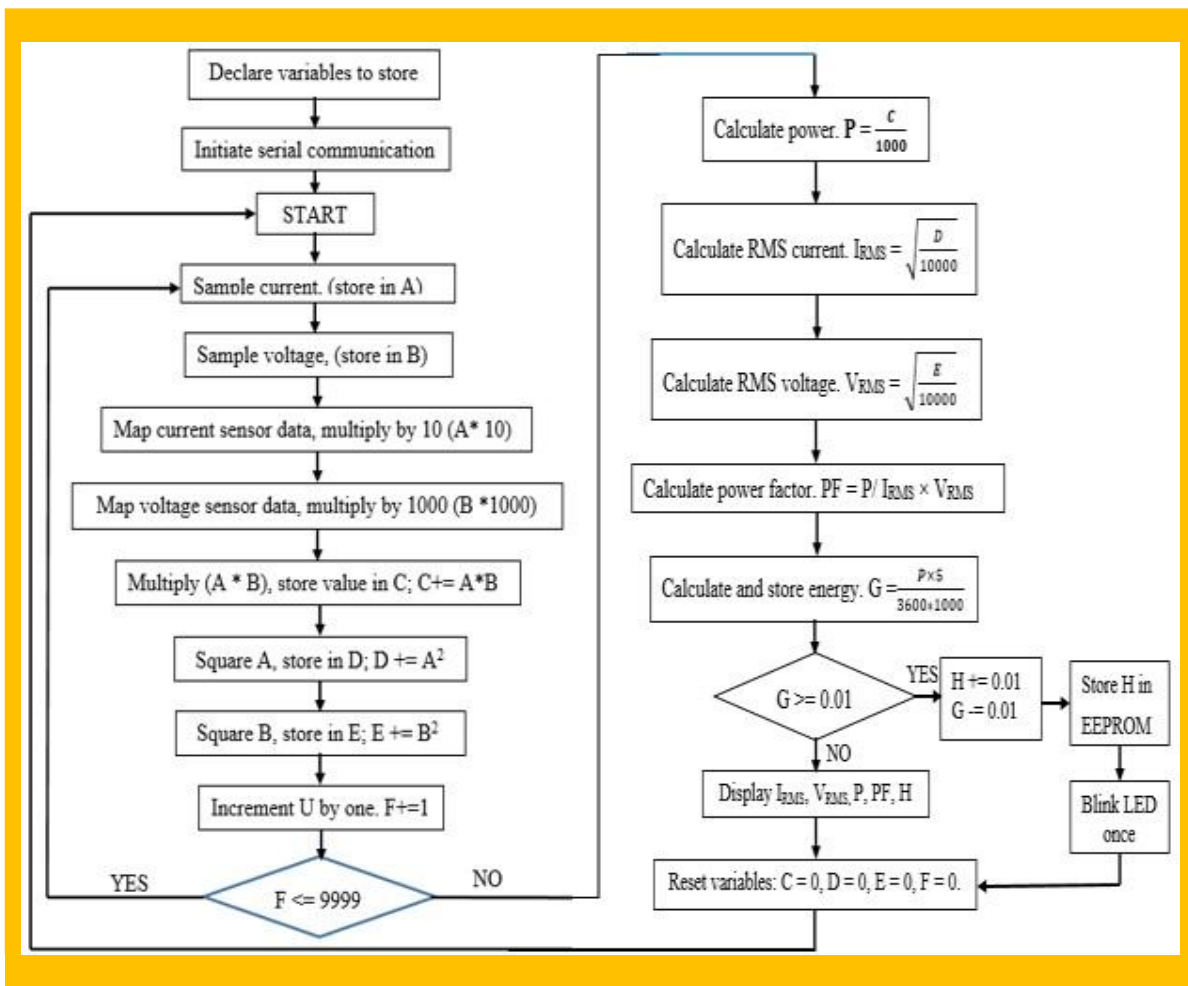


Figure 4: Flow chart for software development

The electrical energy consumed over 10000 samples (in 5 seconds) would be computed and stored in EEPROM. When this value cumulated to 0.01 kWhrs, the LED blinked once and the value was added to the total units consumed. This figure was used in calibrating the designed meter. The cumulative energy units (kWhrs) were displayed on the LCD. The LCD also displayed the current, voltage, power and pf over the 10000 samples after which they were reset to zero. The process was repeated for the following sampling interval(s) until 0.01 kWhrs were consumed. A record of the cumulative kWhr units was stored in the EEPROM and was incremented after a consumption of every 0.01 kWhrs.

### **2.3 Experimental Set-up using Prototype Meter**

The se-up included a single-phase power circuit wired with 2.5 mm<sup>2</sup> PVC sheathed twin with earth flat cable complete with 13A plates. The installation also had 3 single phase lighting circuits each wired with 1.5 mm<sup>2</sup> PVC sheathed twin with earth flat cable completely wired with switched plates, lamp holders and fluorescent fittings. The whole installation was protected by circuit breakers housed in a 6-way consumer unit. The 1.22M×36W fluorescent fittings and 100W bulbs were mounted on a vertically-mounted 1.22M×2.44M block board which also acted as a bright light shield to the researcher. The board, the energy meters and other instruments were arranged on a laboratory bench as shown in Figure 5 where the digital meters and other instruments are placed horizontal or slightly elevated while the electro-mechanical induction type rotating disc energy meter is mounted vertically on the block board.



**Figure 5: Researcher sets up laboratory instruments to carry out experiments**

Figure 6 shows 4 electrical energy meters connected to simultaneously measure electrical energy. In this template, the induction type energy meter is not captured. The reference and prototype energy meters also displayed voltage, current, power, and power factor (the reference meter displayed other variables too).

Figure 7 shows a snap shot of the LCD display in one of the test runs. In this case,  $P = V \times I \times pf = 235 \times 3.30 \times 1.0 = 775.5W$ . The displayed value was 775W which gave a difference of 0.5W while the accumulated energy was 1.06 kWhrs.



**Figure 6: Electrical energy meters under test**



**Figure 7: Snap shot of Prototype meter LCD display of voltage, current, pf, 'real-time' power and electrical energy**

### **3 RESULTS AND DISCUSSION**

This section includes details of experimental work performed on the prototype AMR current sensor and the electrical energy meter designed using the sensor. Data collection was replicated three times and analysed using Statistical Analysis of Systems (SAS, 2001). Statistical data results were used to draw bar graphs and discussions based on the means and Least Significant Different (LSD) at 5% level of significance.

#### **3.1 Current sensor output/input relationship**

A linear regression was performed on the test results of the sensor's output voltage and current flowing through it as shown in Table 2 and Figure 8.

**Table 2: Regression Statistics**

SUMMARY OUTPUT								
Regression Statistics								
Multiple R	0.999993708							
R Square	0.999987416							
Adjusted R Square	0.999986158							
Standard Error	0.000721255							
Observations	12							
ANOVA								
	df	SS	MS	F	Significance F			
Regression	1	0.413381465	0.41338146	794644.35	7.76625E-26			
Residual	10	5.20209E-06	5.2021E-07					
Total	11	0.413386667						
	Coefficients	Standard Error	t Stat	P-value	Lower 95%	Upper 95%	Lower 95.0%	Upper 95.0%
Intercept	0.000600893	0.000412142	1.45797607	0.17552586	-0.000317416	0.001519	-0.0003174	0.0015192
X Variable 1	0.099821316	0.000111979	891.428264	7.7663E-26	0.099571811		0.0995718	0.10007082

The regression line in Table 2 is given by  $V_{out} = 0.000600893 + 0.099821316I$  volts, where the  $V_{out}$ -intercept is 0.000600893, the slope of the regression line is 0.099821316 and  $I$  is the current flowing through the sensor and load. Applying the above equation, the output voltage for a current of 25A is  $V_{out} = 2.496$  volts. The formula for the output voltage of the AMR current sensor may therefore be approximated to  $V_{out} = 0.1I$  volts which agree with the manufacturer's data sheets. The current sensor was found to have a linear relationship between its output voltage and the current flowing through it. It was therefore found to be suitable for the design of an electrical energy meter for the measurement of electrical energy.

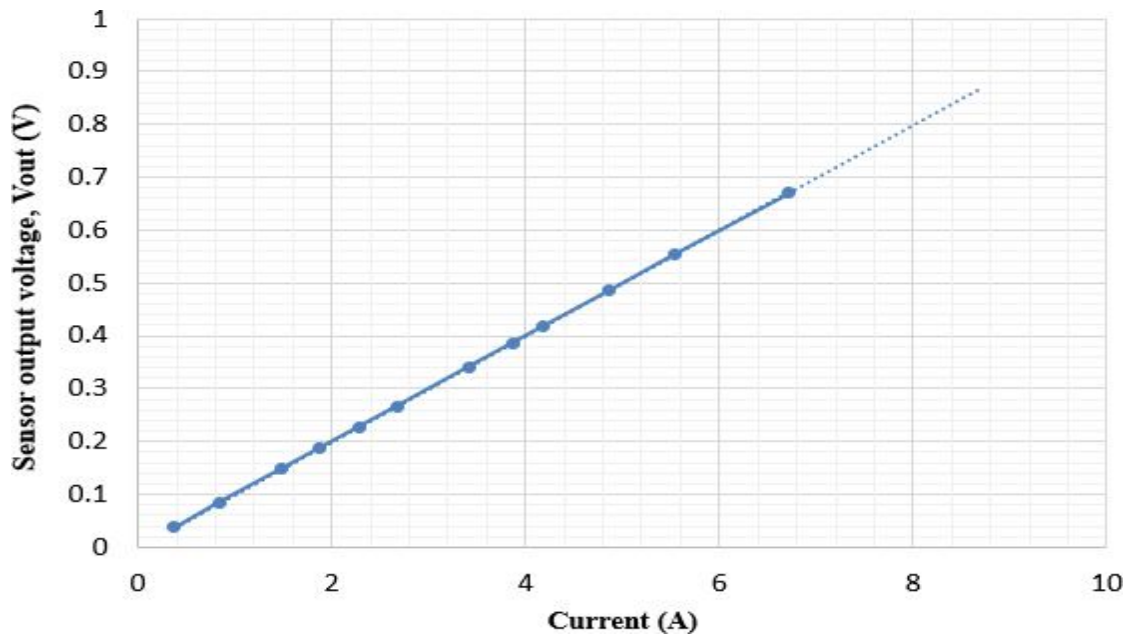


**Figure 8: Linear regression on sensor current and output voltage**

### 3.2 Measurements using the prototype meter

The prototype meter was designed to display the current flowing through the load, the consumer's terminal voltage, the power consumed, the load power factor and the electrical energy consumed. Therefore, the meter had to be tested against other commercial meters to assess its suitability in the measurement of the above variables. The supply was 240V, 50Hz and the loads were combinations of 100W bulbs and 1.22M×36W fluorescent fittings. The test was replicated 3 times and the raw data recorded for one of the loads (L1) is shown in Table 3. This test was repeated for each of the 5 loads and the data analysed using SAS, 2001. The raw data for the other load tests is not shown but analysed data results for those tests are shown.

**Table 3: Measurements of current, voltage, pf, power and electrical energy using load L1 (14×100W incandescent bulbs).**

Time (mins)	Current (A)			Voltage (V)			Power factor		Power (W)		Electrical Energy recorded (kWhrs)				
	I1	IBM	IFM	V1	VBM	VFM	pfBM	pPFM	PBM	PFM	EBM	EFM	EM1	EM2	EM3
0	5.66	5.69	5.61	227	228	228	1	1	1301	1200	0	0	0	0.1	0
5	5.66	5.69	5.61	227	226	227	1	1	1311	1200	0.109	0.11	0.11	0.1	0.11
5	5.65	5.69	5.61	227	226	227	1	1	1310	1200	0.109	0.11	0.11	0.1	0.12
5	5.65	5.69	5.59	227	228	227	1	1	1308	1200	0.109	0.11	0.11	0.1	0.12

It is important to note that the readings were closely and continuously monitored during each replication of 5 minutes. Similar results were obtained using 3 other loads and 4 replications of 5 minutes each. A sampled result of analysed data for current is shown in section 3.2.6.

Accurate measurements of current and voltage by the prototype meter was very important because they directly affected the accuracy of the other related variables. The meter was therefore first tested to assess its accuracy for the measurement of current and voltage. All the meters used to measure the variables had been calibrated by Kenya Bureau of Standards (KEBS). The results were analysed using Statistical Analysis of Systems (SAS, 2001).

#### 3.2.1 Current Measurements

Three types of ammeters were connected to measure the current drawn by the electrical loads. The mean currents are shown in Table 4. The means that have the same letter superscripts in the same columns are not significantly different. In the third and fourth columns (labelled L2 and L3), the means shared the same letter superscripts in the third and fifth rows. This implies that there was no significant difference between the means. In the first, fourth and fifth columns, there was no sharing of the letter superscripts which implied that there was a significant difference between the means. This implied that the three meters had differences in their readings.

**Table 4: Current means measured by ammeters on various electrical loads.**

Ammeters	Electrical Loads				
	L1	L2	L3	L4	L5
Reference - IBM(A)	5.690 <sup>a</sup>	4.44 <sup>b</sup>	7.05 <sup>b</sup>	3.335 <sup>a</sup>	6.16 <sup>b</sup>
Lab Meter - I1(A)	5.657 <sup>b</sup>	4.55 <sup>a</sup>	7.23 <sup>a</sup>	3.33 <sup>b</sup>	6.17 <sup>a</sup>
Prototype - IFM(A)	5.603 <sup>c</sup>	4.44 <sup>b</sup>	7.05 <sup>b</sup>	3.31 <sup>c</sup>	6.07 <sup>c</sup>

*NB: Current means followed by the same letter superscripts (a, b or c) in the respective columns are not significantly different at  $\alpha = 0.05$ .*

To compare the performance of the prototype meter with others, collected test data was plotted in Figure 9 and error bars inserted. The reference (POWERTEK), laboratory and prototype ammeters represented by IBM, I1 and IFM on the chart indicate analysed current. The error bars overlapped in all the 5 load tests which implied that the means of the currents were not significantly different and that the prototype meter performed well compared with the other ammeters.

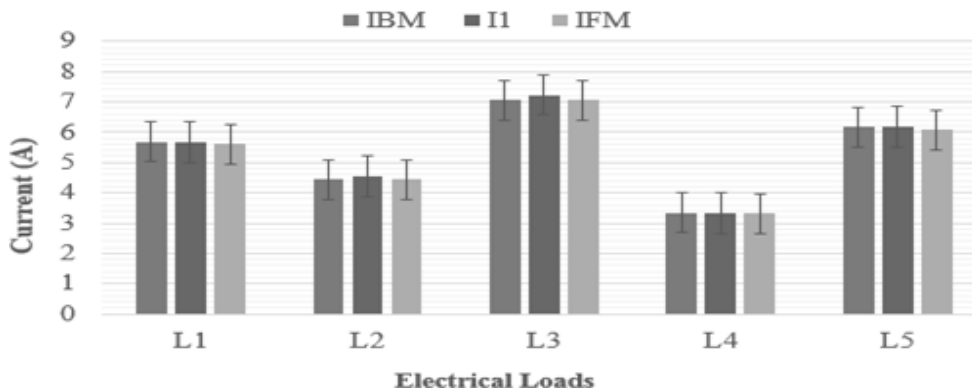


**Figure 9: Measurements of currents on various electrical loads**

### 3.2.2 Voltage Measurements

Three voltmeters were connected to measure the terminal voltages. VBM, VFM and V1 represent the analysed voltage means measured using the reference (POWERTEK), prototype and laboratory voltmeters, respectively. The results were analysed using Statistical Analysis of Systems (SAS, 2001). The mean voltages are tabulated in Table 5. The voltage means that have the same letter superscripts in the respective columns are not significantly different.

**Table 5: Voltage means measured by voltmeters on various electrical loads.**

Voltsmeters	Electrical Loads				
	L1	L2	L3	L4	L5
Reference - VBM(V)	226.67 <sup>a</sup>	231.67 <sup>a</sup>	229.67 <sup>a</sup>	236 <sup>a</sup>	232.67 <sup>a</sup>
Lab Meter - V1(V)	227 <sup>a</sup>	230.33 <sup>b</sup>	227.67 <sup>b</sup>	233.33 <sup>c</sup>	230.33 <sup>b</sup>
Prototype - VFM(V)	227 <sup>a</sup>	231.67 <sup>a</sup>	229.33 <sup>a</sup>	235 <sup>b</sup>	232.33 <sup>a</sup>

*NB: Voltage means followed by the same letter superscript (a, b or c) in the respective columns are not significantly different at  $\alpha = 0.05$ .*

In the second column (Electrical load L1), the voltage means for the three voltmeters shared the same letter superscripts implying that the voltage means were not significantly different. However, the voltage means for the loads (L2, L3 and L5) had similar behaviours though load L4 was slightly different from the rest. Reference VBM(V) and Prototype VFM(V) voltmeters had similar performance since their voltage means had the same superscript except for load L4 which did not share the same superscript.

Also, to ascertain the performance of the prototype meter with the other two voltmeters, the data was plotted as in Figure 10 and error bars inserted. The error bars overlapped on all the 5 load tests which implied that the voltage means of the 3 voltmeters were not significantly different in all the tests and that the prototype meter performed well against the reference and laboratory voltmeters.

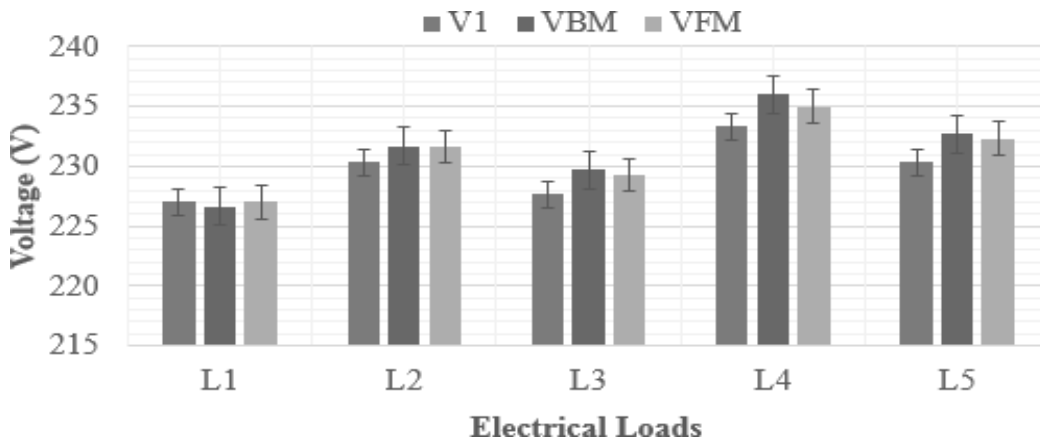


**Figure 10: Voltage versus Electrical Loads**

### 3.2.3 Electrical Energy Measurements

The electronic meter labelled „EM1“ had a current transformer sensor while „EM3“ was an induction electro -mechanical rotating disc type (English Electric) energy meter. To test the AMR prototype meter, 4 meters were connected to measure electrical energy consumed by 5 electrical loads for 5 minutes each and replicated 3 times. Ammeters and voltmeters were also connected to measure the load currents and the terminal voltages. The energy measurement from the reference meter was obtained indirectly by multiplying its power reading (observed to be constant during the test) with a selected consumption period of 5 minutes recorded using an electronic timer. The results showing the means of electrical energies from the 4 electrical energy meters are shown in Table 6. The energy means in the fifth and sixth columns were followed by the same letter superscripts which implied that they were not significantly different at 5% significance level. The other superscripts were different implying that the means were significantly different.

**Table 6: Electrical energy means in kWhrs**

Energy meters	Electrical Loads				
	L1	L2	L3	L4	L5
Reference - EBM	0.109 <sup>b</sup>	0.083 <sup>c</sup>	0.134 <sup>b</sup>	0.067 <sup>a</sup>	0.1197 <sup>a</sup>
Prototype - EFM	0.11 <sup>ab</sup>	0.093 <sup>ab</sup>	0.143 <sup>ab</sup>	0.07 <sup>a</sup>	0.123 <sup>a</sup>
Electronic - EM1	0.107 <sup>b</sup>	0.087 <sup>bc</sup>	0.157 <sup>a</sup>	0.067 <sup>a</sup>	0.123 <sup>a</sup>
Induction - EM3	0.117 <sup>a</sup>	0.097 <sup>a</sup>	0.157 <sup>a</sup>	0.07 <sup>a</sup>	0.133 <sup>a</sup>

*NB: Electrical energy means followed by the same letter superscript (a, b or c) in the respective columns are not significantly different at  $\alpha = 0.05$ .*

To compare the performance of the energy meters, the means were plotted in Figure 11 and standard error bars included. It was observed that all the error bars overlapped. This implied that the performances of the energy meters were not significantly different and that the prototype meter performed well against the reference meter. The electro-mechanical induction type energy meter, which is quickly being replaced with the electronic meters, also performed well.

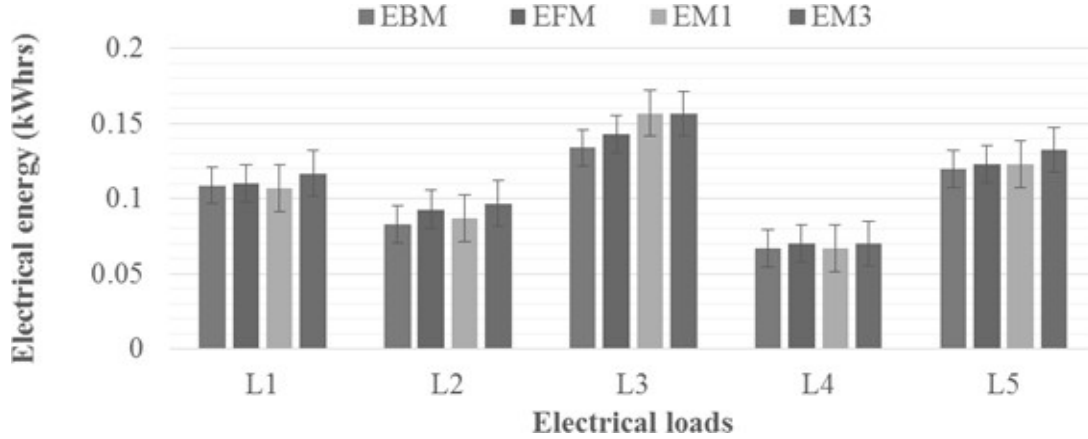


**Figure 11: Electrical Energy versus electrical Loads**

### 3.2.4 Power Measurement

The reference and prototype meters were used to measure the power consumed by the 5 loads and their means are shown in Table 7. It was observed that the letter superscripts following the means in all the columns (except column 3) were not the same and therefore the means were significantly different. This means that the meters recorded different readings.

**Table 7: Power means in Watts**

Wattmeters	Electrical Loads				
	L1	L2	L3	L4	L5
Reference - PBM(W)	1309.67 <sup>a</sup>	994.3 <sup>a</sup>	1612 <sup>a</sup>	792.67 <sup>a</sup>	1436.67 <sup>a</sup>
Prototype – PFM(W)	1280.0 <sup>b</sup>	1002 <sup>a</sup>	1606.67 <sup>b</sup>	778.67 <sup>b</sup>	1410.0 <sup>b</sup>

*NB: Power mean values followed by the same letter superscript (a or b) in the respective columns are not significantly different at  $\alpha = 0.05$ .*

To compare the performance of the power meters, the means were plotted in Figure 12 and standard error bars included. It was observed that all the error bars overlapped. This implied that the performances of the „power factor“ meters were not significantly different. It was observed that the prototype meter performed well against the reference meter.

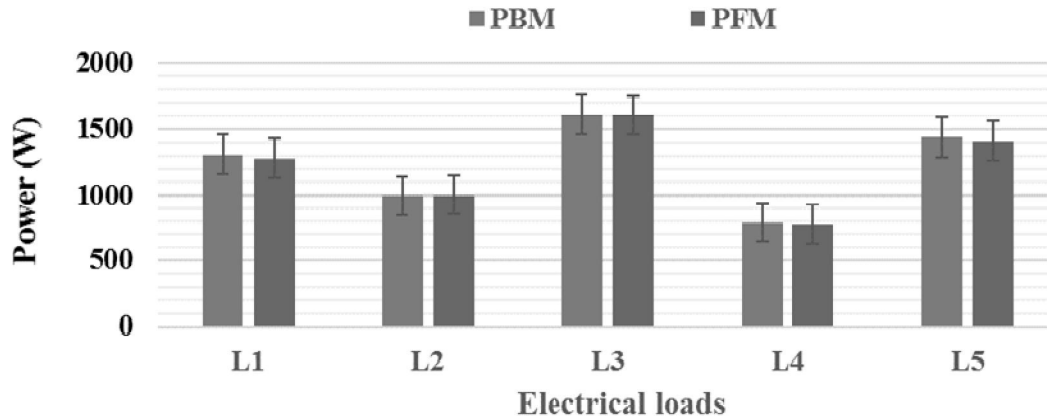


**Figure 12: Power measured using two wattmeters on different loads**

### 3.2.5 Power Factor Measurement

The reference and prototype meters were used to measure the consumer's power factor (pf) and the means are as shown in Table 8. It was observed that the letter superscripts following the means in all the columns (except one) were the same and therefore the means were not significantly different. This implies that the two meters displayed similar readings in almost all the cases. It was also realised that the two meters displayed correct figure of unity pf as expected for resistive loads.

**Table 8: Power factors mean values**

Power Factor meters	Electrical Loads				
	L1	L2	L3	L4	L5
Reference - pfBM	1.0 <sup>a</sup>	0.94 <sup>a</sup>	0.98 <sup>b</sup>	1.0 <sup>a</sup>	1.0 <sup>a</sup>
Prototype - pfFM	1.0 <sup>a</sup>	0.96 <sup>a</sup>	0.99 <sup>a</sup>	1.0 <sup>a</sup>	1.0 <sup>a</sup>

*NB: Power factor means followed by the same letter superscript (a or b) in the respective columns are not significantly different at  $\alpha = 0.05$ .*

To compare the performance of the power factor (pf) meters, the data in Table 6 was plotted in Figure 13 and error bars inserted. It was observed that the error bars overlapped for all the loads. This implied that the prototype meter competed well against the reference meter.

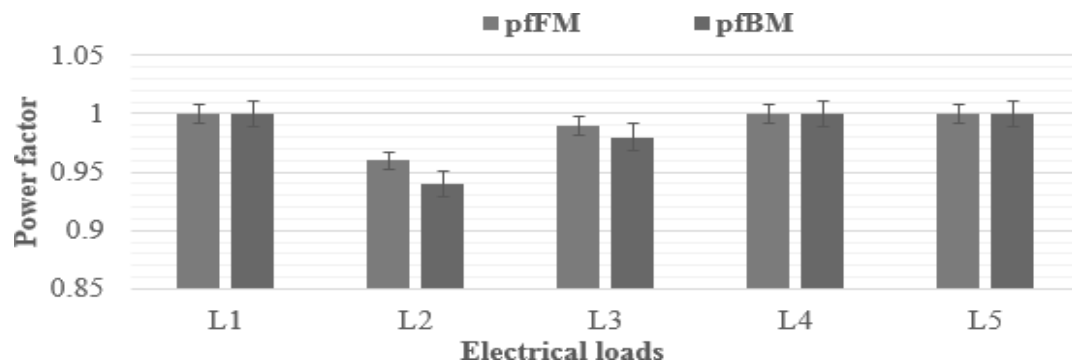


**Figure 13: Power factor measured with the reference and prototype meters**

### 3.2.6 Prototype Meter Testing using 3 Electrical Loads

This section presents the performance of the prototype AMR meter in the measurement of various electrical variables but only discusses in detail the measurement and analysis of current. The meter was tested using 3 electrical loads with each load test lasting 5 minutes and replicated 4 times. The raw data for the supply current, voltage, power consumed, pf and electrical energy are given in Table 9 for a load of 5×36W fluorescent fittings. The data for the other 2 load tests using loads L1 and L2 were recorded in similar Tables (5×36W 1.22M fluorescent fittings plus 6×100 Watt bulbs and 5×36W 1.22M fluorescent fittings plus 14×100 Watt bulbs respectively).

**Table 9: Raw Data for Electrical Load L1 of 5×36W fluorescent fittings**

Time (mins)	Current (A)				Voltage (V)			Power factor		Power (W)		Electrical Energy recorded (kWhrs)					Blinks
	I1	IBM	IFM	I4	V1	VBM	VFM	pfBM	pfFM	PBM	PFM	EBM	EFM	EM1	EM2	EM3	
0	1.77	1.83	1.8	1.72	230	232	231	0.5	0.57	210	234	0	0	0	0	0	
5	1.76	1.8	1.77	1.71	230	231	230	0.51	0.58	211	234	0.0176	0.02	0.02	0	0.01	2
5	1.75	1.79	1.76	1.72	230	231	230	0.51	0.58	210	232	0.0175	0.02	0.02	0	0.02	2
5	1.71	1.74	1.73	1.65	228	230	228	0.52	0.58	212	233	0.0177	0.02	0.02	0	0.02	2
5	1.72	1.76	1.74	1.66	229	230	229	0.52	0.59	212	233	0.0177	0.02	0.02	0.1	0.02	2

The analysed data presented in Table 10 show that the means in the same column were not followed by the same letter superscripts which implied that the meters had different readings. However, in 2 columns, some means were followed by the same letter superscripts which implied that there was no significant difference between the meter readings.

**Table 10: Means of currents measured on different instruments for loads L1, L2 and L3**

Ammeter currents	Electrical Loads		
	L1	L2	L3
IBM	1.773 <sup>a</sup>	3.63 <sup>b</sup>	6.75 <sup>a</sup>
IFM	1.750 <sup>b</sup>	3.58 <sup>c</sup>	6.64 <sup>b</sup>
I1	1.735 <sup>c</sup>	3.66 <sup>a</sup>	6.76 <sup>a</sup>
I4	1.685 <sup>d</sup>	3.66 <sup>a</sup>	6.76 <sup>a</sup>

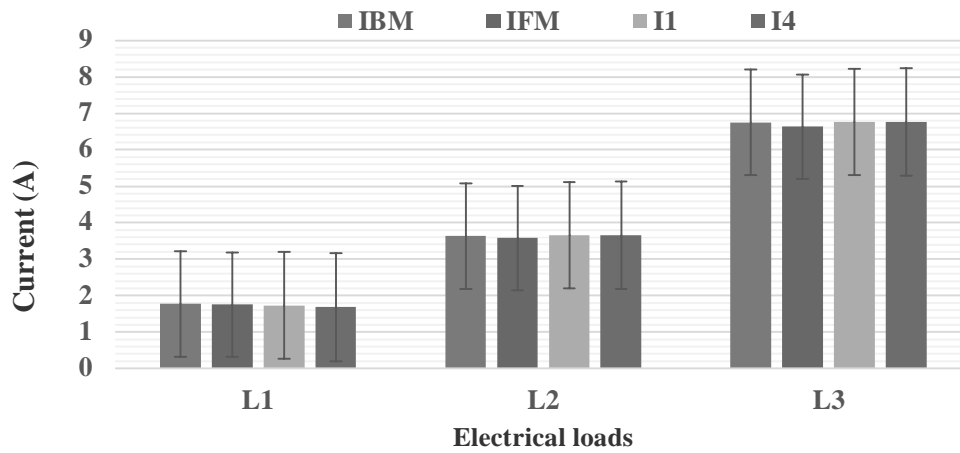
*Means followed by the same letter in the same column are not significantly different at 0.05 level of significance and LSD of .0001*

The ANOVA Summary for current presented in Table 11 shows that all the R-Square values were almost unity (above 0.97) which was a good indication that the data clustered closely to the overall mean. The p-values for loads L1, L2 and L3 were lower than the significance level of 0.05. This implied that the differences between the means were significantly different. This was in agreement with the results in Table 10 which shows that the means did not share same letter superscripts in the same columns for the 3 loads.

**Table 11: ANOVA Summary for Current**

Load	R-Square	Coeff. Var	Root MSE	Mean Current	F Value	LSD
L1	0.973952	0.491991	0.008539	1.735625	75.51	<.0001
L2	0.971382	0.271723	0.009860	3.628750	62.66	<.0001
L3	0.970393	0.202897	0.013642	6.723750	76.07	<.0001

To compare the performance of the meters in the measurement of current, the data in Table 10 was plotted in Figure 14 and standard error bars included. It was observed that all the error bars overlapped implying that the mean currents were not significantly different. This was an indication that the performance of the ammeters was not significantly different. Since all the error bars of the prototype AMR meter overlapped with the others, it implied that the performance of the meter was not significantly different from that of the other meters. Similar analysis and discussions were carried out for voltage, power consumed, and electrical energy.

**Figure 14: Current drawn by different loads measured on various ammeters**

#### 4 CONCLUSION

Since the AMR current sensor had a linear output/input relationship, it was considered suitable for metering electrical energy. The formula gave an output of 2.496V for a current of 25A which agreed with the manufacturer's figure of 2.5V for the same current.

Statistical results were used to determine the performance of the prototype meter in comparison with other meters for the measurement of electrical energy. The performance of the prototype meter on current, voltage, power consumption and power factor indicated that its performance was not significantly different from those of the other meters. The results from the bar graphs revealed that the error bars of the prototype overlapped with the other error bars in all the experiments. This implied that their performances were not significantly different. The results showed that the AMR current sensor is a competitive candidate of choice in electrical energy metering.

Additionally, the prototype meter also displayed current, voltage, power consumption and power factor which are not normally displayed by the other meters. If the consumers were to frequently observe their meter readings, report cases of under-voltages, switch off unnecessary large power-consuming loads and improve their power factors, their supply service would not only be improved but they would also pay reduced electricity bills. The displayed information would also directly assist the service providers to quickly assess the customers' load demands, performance of their power distribution systems and feedback on their system upgrades.

### Recommendations

Tests carried out on the AMR current sensor showed that there was a substantial error at low input currents (about 6% at 0.5A) which declined to within 1% at about 1.8A. However, the error remained within  $\pm 1\%$  at current values above 1.8A. If, in the manufacture of the current sensor, barber poles were arranged to improve the accuracy at low currents, the sensor would be more suitable for low current measurements. The prototype meter should therefore be studied further to investigate how this error could be reduced at load currents below 1.8 A.

### References

1. Seal, B. & McGranaghan, M. (2010). Accuracy of Digital Electricity Meters, *Electric Power Research Institute (EPRI)*, Inc. Retrieved from <http://www.epri.com>.
2. Nwagbo C. L. and Baah B., (2022). A comparative study of basic types of energy meters and metering. *Global Journal of Engineering and Technology Advances*, 10(01), 117–124.
3. Aswathi M, Gandhiraj R, Soman K, (2015). Application and Analysis of Smart Meter Data along with RTL SDR and GNU Radio. *Procedia Technology* 21, pp. 317 – 325
4. Haque M, Hossain K, Ali M, Sheikh R. I (2011). Microcontroller Based Single Phase Digital Prepaid Energy Meter for Improved Metering and Billing System. *International Journal of Power Electronics and Drive System (IJPEDS)*, 1(2), pp. 139~147
5. Shomuyiwa, D.A. & Ilevbare, J.O. (2013). Design and Implementation of Remotely-Monitored Single Phase Smart Energy Meter via Short Message Service (SMS). *International Journal of Computer Applications*, 74(9), pp. 0975 – 8887.
6. Arun, S. & Naidu, S. (2012). Hybrid Automatic Meter Reading System. *International Journal of Advanced Research in Computer Science and Software Engineering*, 2(7).
7. Zahurul S, Mariun N, Grozescu V, Lutfi M L, Hizam H, Abidin I Z (2013). Electricity Measurement Sensor: A Review on Application to Smart Meter Communication. *International Conference on Engineering Education*.
8. Al-Omary, A., El-Medany, W. & Al-Irhayim S. (2011). Design and Implementation of Secure Low Cost Automatic Meter Reading System using GPRS Technology. *International Conference on Telecommunication Technology and Applications*, Proc of CSIT, Vol.5, IACSIT Press, Singapore.
9. Koon,W. (1999). *Current Sensing For Energy Metering*. Retrieved from <http://www.analog.com>
10. Ashiquzzaman Md, Afroze N. & Abdullah Md. T. (2012). Design and Implementation of Wireless Digital Energy Meter using Microcontroller. *Global Journal of Researches in Engineering (F)*, 12(2).
11. Volokhin, V. & Diahovchenko, I. (2017). Peculiarities of current sensors used in contemporary electric energy metering devices. *ENERGETIKA*, pp.. 8-15.

12. Cetina, Q, Andrew, Roscoe A. J, & Wright P.S. (2017). A Review of Electrical Metering Accuracy Standards in the Context of Dynamic Power Quality Conditions of the Grid. *IEEE*.
13. Shahrara, R. (2011). *Design and Implementation of a Microcontroller Based Wireless Energy Meter*, (Master of Science in Electrical and Electronic Engineering), Eastern Mediterranean University, Gazimağusa, North Cyprus.
14. Hou, F. and Yu, P. (2011). Implementation of a Single-Phase Electronic Watt-Hour Meter Using the MSP430AFE2xx. Application report.
15. Hribik. J., Fuchs. P., Hruškovic. M., Michálek. R. & Lojko B. (2004). Digital Power and Energy Measurement. *Measurement Science Review*, 4(3), 17.
16. Kamilaris, A. (2012). Enabling Smart Homes Using Web Technologies. (PhD Dissertation), University of Cyprus, Cyprus.
17. Yan S., Zhou Z., Yang Y., Leng O., and Zhao W. (2022). Developments and Applications of Tunneling Magneto-resistance Sensors. *Tsinghua Science and Technology*, Volume 27.
18. Enrique G.V, Diego R.M, Sergio I.R.A, Jaime S.M, Susana C, Ricardo F, and Paulo F, (2017). Electronic Energy Meter Based on a Tunnel Magneto-Resistive Effect (TMR) Current Sensor. *Materials* - 10, 1134
19. Ziegler S., Robert, C., Woodward, H., Ho-Ching I., & Lawrence, J. B. (2009). Current Sensing Techniques. *IEEE Sensors Journal*, 9(4).
20. Friedrich, A.P, & Kunze, J, (2000). Universal Magneto-resistive Current Sensor for Automotive Applications, *Publication by SENSiTEC GmbH*, ImAmtmann 6, 6330 Wetzlar-Blankenfeld, Germany.
21. Pinto, J.G.O. & Afonso, J.L. (2006). Development of a Low Cost Digital Energy Meter, *3<sup>rd</sup> International Conference on Hands-on Science - Science Education and Sustainable Development*, University of Minho, Braga, Portugal.